Research Square

Preprints are preliminary reports that have not undergone peer review.
They should not be considered conclusive, used to inform clinical practice,
or referenced by the media as validated information.

Oblique Fixation from Posterior Corner in Lumbar Spine Through Kambin's Triangle: A Neuroimaging Anatomic Assessment

Feifei Chen
Shandong Provincial Hospital Affiliated to Shandong University

Jun Xin
Department of Spine Surgery, Shandong Provincial Hospital Affiliated to Shandong University, Shandong Provincial Hospital Affiliated to Shandong First Medical University, No.9677, Jingshi Road, Jinan City,China

Cheng Su
Department of Spine Surgery, Shandong Provincial Hospital Affiliated to Shandong University, Shandong Provincial Hospital Affiliated to Shandong First Medical University, No.9677, Jingshi Road, Jinan City,China

Jianmin Sun
Department of Spine Surgery, Shandong Provincial Hospital Affiliated to Shandong University, Shandong Provincial Hospital Affiliated to Shandong First Medical University, No.9677, Jingshi Road, Jinan City,China

Xiaoyang Liu
Department of Spine Surgery, Shandong Provincial Hospital Affiliated to Shandong University, Shandong Provincial Hospital Affiliated to Shandong First Medical University, No.9677, Jingshi Road, Jinan City,China

Xingang Cui (spine2014@163.com)
Department of Spine Surgery, Shandong Provincial Hospital Affiliated to Shandong University, Shandong Provincial Hospital Affiliated to Shandong First Medical University, No.9677, Jingshi Road, Jinan City,China

---

Research

Keywords: Lumbar spine, Posterior corner, Oblique fixation, Kambin's triangle, Imaging anatomy

Posted Date: May 13th, 2020

DOI: https://doi.org/10.21203/rs.3.rs-28077/v1

License: This work is licensed under a Creative Commons Attribution 4.0 International License.
Read Full License

Abstract

Background: Traditional lumbar interbody fusion has many limitations, such as large trauma, severe damage to the normal posterior structure, and long postoperative recovery period. With the advance of minimally invasive surgery and spinal endoscopy, new fusion technologies such as percutaneous endoscopic transforaminal lumbar interbody fusion (PE-TLIF) and endoscopic transforaminal lumbar interbody fusion (Endo-LIF) through Kambin's triangle with less trauma, less bleeding and faster recovery have been developed. However, nerve root injury and dural tears are important complications, and Kambin's triangle is not "safe". Moreover, fusion after decompression often requires placement of a 14-mm channel, removal of more articular processes, fixation with posterior percutaneous pedicle screw, and changes of intraoperative position or anesthesia, which are inconvenient. One-stop percutaneous endoscopic transforaminal oblique fixation from posterior corner in lumbar spine overcomes the above limitations, and realizes one-stop decompression, fusion and fixation in a single regular minimally invasive channel. The purpose of this study is to measure the neuroimaging anatomic parameters of the nerves related to oblique fixation from posterior corner in lumbar spine through Kambin's triangle, to define and evaluate the safe working area in Kambin's triangle, and to identify the optimal target area for endoscopic fusion and fixation.

Methods: Sixty volunteers (27 males and 33 females) underwent lumbar MR examination (VISTA,3D-STIR-TSE Sequence) and the data were uploaded to Philips (Achieva 1.5T MR) workstation. Three working targets (P1, P2, P3) were preset for oblique fixation from posterior corner in lumbar spine. The distances from the working targets to exiting nerve roots and dural sac/traversing nerve roots in the coronal and sagittal planes, and the distances from the exiting roots to the dural sac/traversing nerve roots in the upper and lower endplate planes were measured and statistically analyzed.

Results: In L1/2–L5/S1, the *P* values of paired *t*-test for the distances (c1, c2, c3, c4, c5 and c6) from each target (P1, P2 and P3) to the ipsilateral exiting nerve roots and dural sac/traversing nerve roots were all greater than 0.05. There were no statistically significant differences between the targets at both sides of the same segment, and the mean values of both sides were calculated. The c1, c2, c3, c4, c5 and c6 all increased and then decreased, gradually increased from L1/2, maximized in L4/5, and decreased slightly in L5/S1. As the targets (P1, P2, P3) moved laterally along the horizontal midline of the posterior margin of intervertebral disc, the distance to the dural sac/traversing nerve roots gradually increased, while the distance to the exiting roots gradually decreased. The distance from P1 to exiting nerve roots was significantly greater (1–3 mm) than that to dural sac/traversing nerve roots. The distance from P3 to exiting nerve roots was significantly smaller (1–3 mm) than that to dural sac/traversing nerve roots. The distances from P2 to exiting nerve roots and to dural sac/traversing nerve roots did not different significantly in each segment, and the differences in means were within 1 mm.

The distances from exiting nerve roots to dural sac/traversing nerve roots in the upper and lower endplate planes (d1, d2) gradually increased in L1/2–L5/S1 ($P<0.0001$) and the means of d2 were greater than d1

(P<0.05). There was no statistically significant difference between the left and right sides in the upper and lower endplates in each segment (P=0.26).

In L1/2–L5/S1, the P values of paired t-test for the distances (s1, s2, s3, s4, s5, s6) from the projection points of posterior-inferior (posterior-superior) corner of upper (lower) vertebral body to exiting nerve roots in the sagittal planes passing the targets were all greater than 0.05. There was no statistically significant difference between both sides of the same segment, and thus the mean value was calculated. With the outward shift of the targets in the sagittal planes, s1, s3 and s5 gradually decreased (s1>s3>s5), and the same trend was found for s2, s4 and s6 (s2>s4>s6). The distances gradually increased in each segment from the smallest value in L1/2 to the largest value in L5/S1.

Conclusion: Kambin's triangle can be used as a working area for oblique fixation from posterior corner in lumbar spine, but the actual safe area is smaller than theoretical prediction. The intersection point between the vertical line from the medial 1/3 of pedicle and the horizontal midline of the posterior margin of intervertebral disc (P2) is an ideal "target" for oblique fixation from posterior corner in lumbar spine. It is neuroanatomically feasible to achieve one-stop complete decompression, fusion, and fixation in a single channel under spinal endoscopy. Further biomechanical studies and clinical trials are needed to determine whether it can be a new option for posterior spinal fusion.

Background

Lumbar interbody fusion surgery has become a standard operation in the treatment of various degenerative lumbar diseases [1], mostly through the posterior approach. Traditional lumbar interbody fusion techniques, such as posterior lumbar interbody fusion, transforaminal lumbar interbody fusion, and oblique lumbar interbody fusion, have been widely used due to complete decompression, firm fixation and confirmed efficacy. However, the destruction of the paraspinal muscle, blood vessels, and nerves during operation has resulted in many postoperative complications [2].

At present, PE-TLIF and Endo-LIF through Kambin's triangle have attracted great interest due to less trauma, less bleeding, faster recovery, higher safety and fewer complications. However, they also suffer from drawbacks of incomplete decompression, steep learning curve, low fusion rate and high radiation risk [3–7]. In particular, injury to the traversing nerve roots and the dural sacs leads to aggravated nerve injury and leakage of cerebrospinal fluid. Fusion after decompression often requires placement of a 14-mm channel, removal of more articular processes, fixation with posterior percutaneous pedicle screw, and changes of intraoperative position or anesthesia, which are inconvenient. One-stop percutaneous endoscopic transforaminal oblique fixation from posterior corner in lumbar spine overcomes the above drawbacks, and realizes one-stop decompression, fusion and fixation in a single regular minimally invasive channel (Fig. 1).

The purpose of this study is to measure the neuroimaging anatomic parameters of the nerves related to oblique fixation from posterior corner in lumbar spine through Kambin's triangle, to verify its anatomical

feasibility, to define and evaluate the actual safe working area in Kambin's triangle, and to identify the optimal target area for endoscopic fusion and fixation.

Materials And Methods

Materials

Sixty normal adult volunteers (22 males and 38 females; 20–75 years of age, mean age 37.8 years; male height 168–182 cm, mean 174.6 cm; female height 157–171 cm, mean 165.3 cm; without lumbar tumors, trauma, deformity or a history of lumbar surgery) underwent MR scan (VISTA,3D-STIR-TSE Sequence) of the lumbar spine (Philips Achieva 1.5T MR) in the East Hospital of Shandong Provincial Hospital from December 1, 2019 to February 29, 2020. Scan data were transmitted to the workstation for measurement.

Data Measurement

In oblique fixation from posterior corner in lumbar spine, three points were preset as targets to measure the distances from each target to exiting nerve roots and dural sac/traversing nerve roots, to select the ideal "target", and to indirectly define the safe operation area of oblique fixation from posterior corner in lumbar spine. The three targets were:

P1: the intersection point between the vertical line of inner margin of pedicle and the horizontal midline of the posterior margin of intervertebral disc.

P2: the intersection point between the vertical line from the medial 1/3 of pedicle and the horizontal midline of the posterior margin of intervertebral disc.

P3: the intersection point between the vertical line from the center of pedicle and the horizontal midline of the posterior margin of intervertebral disc.

Data to be measured in the coronary plane: (Figs. 2, 3)

c1: the distance from P1 to ipsilateral exiting nerve roots

c2: the distance from P1 to ipsilateral dural sac/traversing nerve roots

c3: the distance from P2 to ipsilateral exiting nerve roots

c4: the distance from P2 to ipsilateral dural sac/traversing nerve roots

c5: the distance from P3 to ipsilateral exiting nerve roots

c6: the distance from P3 to ipsilateral dural sac/traversing nerve roots

d1: the distance from exiting nerve roots to dural sac/traversing nerve roots in the upper endplate plane

d2: the distance from exiting nerve roots to dural sac/traversing nerve roots in the lower endplate plane

Data to be measured in the sagittal plane: (Figs. 4, 5)

s1: the distance from posterior-inferior corner projection point of upper vertebral body to exiting nerve roots in the sagittal plane passing P1

s2: the distance from posterior-superior corner projection point of lower vertebral body to exiting nerve roots in the sagittal plane passing P1

s3: the distance from posterior-inferior corner projection point of upper vertebral body to exiting nerve roots in the sagittal plane passing P2

s4: the distance from posterior-superior corner projection point of lower vertebral body to exiting nerve roots in the sagittal plane passing P2

s5: the distance from posterior-inferior corner projection point of the upper vertebral body to exiting nerve roots in the sagittal plane passing P3

s6: the distance from posterior-superior corner projection point of lower vertebral body to exiting nerve roots in the sagittal plane passing P3

Statistical Methods

The data were compared with independent sample *t*-test in SPSS 25.0.

Results

Distances from targets to ipsilateral exiting and dural sac/traversing nerve roots in the coronary plane (Table 1)

Distances from targets to ipsilateral exiting nerve roots

In L1/2–L5/S1, the *P* values of paired *t*-test for the distances (c1, c3, c5) from each target to the ipsilateral exiting nerve roots were all greater than 0.05. There were no statistically significant differences between both sides of the same segment, and thus the mean values of both sides were calculated. The distances from P1 to ipsilateral exiting nerve roots in L1/2–L5/S1 were (4.39±0.53), (5.13±0.70), (6.08±0.83), (7.63±0.63), and (7.62±0.91) mm, respectively. The distances from P2 to ipsilateral exiting nerve roots in L1/2–L5/S1 were (4.03±0.77), (4.69±0.66), (5.17±0.93), (6.18±0.90), and (5.49±0.55) mm, respectively. The distances from P3 to ipsilateral exiting nerve roots in L1/2–L5/S1 were (3.67±0.61), (4.16±0.43), (4.54±0.88), (5.39±0.78), and (4.49±0.59) mm, respectively. The c1, c3, and c5 all first increased and then decreased; they gradually increased from L1/2, maximized in L4/5, and decreased slightly in L5/S1. Except for P3 in L1/2, the distances from each target to the exiting nerve roots in each

segment of L1/2–L5/S1 were greater than the conventional working cannula radius (3.75 mm) used in percutaneous endoscopic surgery, which allowed the placement of lumbar interbody fusion cages with cross-sectional diameters of no less than 7.5 mm.

Distances from targets to ipsilateral dural sac/traversing nerve roots

In L1/2–L5/S1, the *P* values of paired *t*-test for the distances (c2, c4, c6) from each target to the dural sac/traversing nerve roots were all greater than 0.05. There were no statistically significant differences between both sides of the same segment, and thus the mean values of both sides were calculated. The distances from P1 to dural sac/traversing nerve roots in L1/2–L5/S1 were (3.75±0.67), (4.25±0.72), (4.65±0.59), (5.49±0.63), and (4.58±0.67) mm, respectively. The distances from P2 to the dural sac/traversing nerve roots in L1/2–L5/S1 were (3.89±0.66), (4.39±0.73), (5.19±0.93), (6.58±0.71), and (6.23±0.97) mm, respectively. The distances from P3 to the dural sac/traversing nerve roots in L1/2–L5/S1 were (4.52±0.53), (5.77±0.33), (5.89±0.77), (7.73±0.80), and (7.67±0.43) mm, respectively. The c2, c4, and c6 all first increased and then decreased; they gradually increased from L1/2, maximized in L4/5, and decreased slightly in L5/S1. The distances from each target to the dural sac/traversing nerve roots in each segment of L1/2–L5/S1 were greater than the conventional working cannula radius (3.75 mm) used in percutaneous endoscopic surgery, which allowed the placement of lumbar interbody fusion cages with cross-sectional diameters of no less than 7.5 mm.

Distances from targets to ipsilateral exiting and dural sac/traversing nerve roots in the coronary plane.

In L1/2–L5/S1, as the targets shifted laterally along the horizontal midline of posterior intervertebral disc, the distances to dural sac/traversing nerve roots gradually increased, while the distances to exiting roots gradually decreased. The distances from P1 to exiting nerve roots were significantly greater than those to dural sac/traversing nerve roots, with differences of 1–3 mm. The distances from P3 to exiting nerve roots were significantly smaller than those to dural sac/traversing nerve roots, with differences of 1–3 mm. However, the distances from P2 to exiting nerve roots and to dural sac/traversing nerve roots did not differ significantly in each segment, and the differences in mean values were within 1 mm. Therefore, we suggest P2 as the optimal target for percutaneous endoscopic transforaminal oblique fixation from posterior corner in lumbar spine.

Distances from the exiting nerve roots to the dural sac/traversing nerve roots in the upper and lower endplate planes in the coronary plane (Table 2)

In L1/2–L5/S1, d1 and d2 gradually increased (F=249.7, P<0.0001; F=511.7, P<0.0001) and d2>d1 (P<0.05). The values of d1 and d2 were the smallest in L1/2 (6.71±2.10; 11.89±2.55) mm and the largest in L5/S1 (13.37±4.09; 22.05±3.96) mm. There was no statistically significant difference between the left and right sides of the upper and lower endplates in each segment.

Distances from posterior-inferior (posterior-superior) corner of upper (lower) vertebral body to exiting nerve roots in the sagittal planes passing the targets (Table 3)

Distances from posterior-inferior corner of upper vertebral body to exiting nerve roots in the sagittal planes passing the targets

In L1/2–L5/S1, the P values of paired t-test for the distances (s1, s3, s5) from posterior-inferior corner of upper vertebral body to exiting nerve roots on the sagittal plane passing the targets were all greater than 0.05. There was no statistically significant difference between the left and right sides of the same segment, and thus the mean values of both sides were calculated. The s1 values in L1/2–L5/S1 were (2.51±0.24), (2.64±0.59), (2.85±0.64), (2.85±0.37), and (3.07±0.82) mm, respectively. The s3 values in L1/2–L5/S1 were (2.65±0.47), (2.72±0.67), (2.86±0.69), (2.93±0.89), and (3.83±0.49) mm, respectively. The s5 values in L1/2–L5/S1 were (3.34±0.80), (3.45±0.27), (3.48±0.99), (3.64±0.46), and (4.75±1.01) mm, respectively. With the outward shift of the targets in the sagittal plane, s1, s3 and s5 gradually decreased (s1>s3>s5). The values gradually increased in segments, with the smallest value in L1/2 and the largest value in L5/S1. We found that the mean values of s1, s3 and s5 in each segment of L1/2–L5/S1 were greater than 2.50 mm, which allowed placement of 5-mm diameter screws to fix the new cage for lumbar interbody fusion.

Distances from posterior-superior corner of lower vertebral body to exiting nerve roots in the sagittal planes passing the targets

In L1/2–L5/S1, the P values of paired t-test for the distances (s2, s4, s6) from posterior-superior corner of lower vertebral body to exiting nerve roots on the sagittal plane passing the targets were all greater than 0.05. There was no statistically significant difference between the left and right sides of the same segment, and thus the mean values of both sides were calculated. The s2 values in L1/2–L5/S1 were (10.04±1.51), (10.15±1.99), (10.25±2.56), (10.66±2.50), and (14.25±2.22) mm, respectively. The s4 values in L1/2–L5/S1 were (7.90±0.65), (8.06±1.25), (8.18±1.42), (8.64±1.17), and (11.65±3.16) mm, respectively. The s6 values in L1/2–L5/S1 were (7.55±0.70), (7.94±1.00), (8.42±1.44), (8.48±1.01), and

(9.10±1.79) mm, respectively. With the outward shift of the targets in the sagittal plane, s2, s4 and s6 gradually decreased (s2>s4>s6). The values gradually increased in segments, with the smallest value in L1/2 and the largest value in L5/S1. We found that the mean values of s2, s4 and s6 in each segment of L1/2–L5/S1 were greater than the diameter (7.5 mm) of conventional working cannula used in percutaneous transforaminal endoscopic surgery, which allowed placement of lumbar interbody fusion cages with cross-sectional diameters of no less than 7.5mm.

Discussion

Advantages of Imaging Measurement

Dry bone or cadaver specimen were used for anatomic measurement because of better visibility and accuracy. However, they suffer from limitations such as difficulty in obtaining specimens, insufficient number of specimens, and destruction of normal anatomical structures in specimen processing that affect the accuracy of measurement. In this paper, we adopted the imaging measurement method to successfully overcome the limitations in the measurement with dry bone and cadaver specimen. We also summarized the advantages of imaging measurement: (1) improvement of measurement efficiency, omission of measuring tools and reading data, which reduces the systematic error and random error to some extent; (2) non-invasive measurement, which preserves object integrity and improves the accuracy of measurement; and (3) sufficient objects can be obtained by imaging measurement.

Development, challenge and thinking of lumbar interbody fusion

Since Hibbs et al first reported the stability of spinal fusion surgery in 1911, and the Mercer proposed that the ideal method of spinal fusion was lumbar interbody fusion in 1936, anterior lumbar interbody fusion and posterior lumbar interbody fusion have achieved promising curative effects [8–13]. However, they suffer from problems like large trauma, high cost, slow recovery, severe damage to normal structures, and postoperative secondary back pain. With the development of minimally invasive concept, the emergence of transforaminal lumbar interbody fusion, extreme lateral lumbar interbody fusion, oblique lumbar interbody fusion, and minimally invasive transforaminal lumbar interbody fusion achieve limited improvement in the disadvantages and deficiencies of traditional open surgery, despite some advances in soft tissue destruction and blood loss.

At present, PE-TLIF and Endo-LIF through Kambin's triangle have attracted much attention due to less trauma, less bleeding, faster recovery, higher safety, and fewer complications. They also have drawbacks such as incomplete decompression, steep learning curve, low fusion rate, high radiation risk [7], and injury to exiting roots and dural sacs, in particular. Lumbar interbody fusion after decompression often requires the use of posterior percutaneous pedicle screws, additional approach and posterior injury, and changes in intraoperative position or anesthesia. Interbody fixation and fusion are often separated and not completed in one process. We propose that, with the help of percutaneous spinal endoscopy, it is possible

to achieve one-stop endoscopic decompression, fusion and fixation in a single minimally invasive channel.

The majority of lumbar interbody fusion surgeries with integrated endoscopy system are performed through the transforaminal approach [14–18]. Anatomical studies have shown that the size of Kambin's triangle in each segment of the lumbar spine is safe for interbody fusion cages [19–20]. The key is how to fully expose and utilize the Kambin's triangle. Lumbar foraminoplasty can remove most of the bone in the superior articular process, fully expose the Kambin's triangle, and provide a safe channel for the placement of fusion cage. However, the place of foraminoplasty should be as far from the exiting nerve roots and as close to the lower half of the intervertebral foramen as possible, so as to obtain sufficient safe space and avoid exiting nerve roots injury [21, 22]. Foraminoplasty close to the apex of superior articular process is likely to cause irritation and even damage to exiting nerve roots [15, 23]. Ozer et al [24] believed that the anatomic variability of Kambin's triangle may be the main reason for nerve root injury in endoscopic spinal surgery. The Kambin's triangle was divided into three types by measuring 34 patients and 8 cadavers. Type I is a closed triangle and there is no available space between sides; type II is a small triangle; and type III is a normal triangle, as described by Kambin. Only 20.8% Kambin's triangles are type III, in which there are wide spaces between the sides. Nearly half (48%) of Kambin's triangles are type II, in which a narrow space exists in the triangle. Nearly one third (31.2%) Kambin's triangles are type I, in which the triangle is closed and there is no space between the sides. Therefore, the Kambin's triangle is not "safe". For one-stop decompression, fusion and fixation in a single minimally invasive channel through the Kambin's triangle, it is necessary to have a new understanding of Kambin's triangle, and to define and evaluate the actual safe working area in Kambin's triangle.

Significance of the actual safe area of Kambin's triangle

Kambin [25] first proposed the concept of "safe triangle" in 1973, therefore, lumbar "safe triangle" is also known as "Kambin's triangle" (Fig. 6A). Kambin's triangle" is a three-dimensional triangle-like structure surrounded by four boundary lines. The lower boundary is the upper endplate of lower vertebral body, the inner boundary is dural sac/traversing nerve roots, the posterior boundary is facet joint, and the outer-upper boundary is exiting nerve roots. Therefore, Kambin's triangle is an irregular wedge-shaped three-dimensional structure, rather than a "triangle". Kambin's triangle was described as a triangular zone surrounded by the upper endplate of lower vertebral body, dural sac/traversing nerve roots, and exiting nerve roots in literature [26–27]. Luis M et al [28] pointed out that Kambin's triangle is not a two-dimensional but a three-dimensional structure, and should not be simply called triangle, and a more appropriate description is "expanded transforaminal corridor", especially in the removal of articular process, pars interarticularis, and lamina. (Fig. 6B)

For decades, Kambin's triangle has been considered to be a relatively safe working area [29]. Spinal surgeons have successively reported transforaminal lumbar interbody fusion, minimally invasive transforaminal lumbar interbody fusion, and endoscopic translaminar lumbar interbody fusion, which are lumbar interbody fusion through Kambin's triangle with safe pass and sufficient operating space [30–33].

Hoshide R et al [34] studied the inner area of lumbar Kambin's triangle. The areas in L1/2–L5/S1 were (66.82 ± 13.89), (90.95 ± 21.29), (127.07 ± 33.43), (167.99 ± 27.64), and (153.75 ± 31.91) mm^2, respectively, which are all larger than the cross-sectional area (44.16 mm^2) of conventional working cannula (7.5 mm diameter) used in transforaminal endoscopic surgery. Since the cross-section of working cannula is circular, the corner of the triangle cannot be regarded as "operable" area, that is, there is a "invalid area" in Kambin's triangle. Therefore, the distances from the preset targets to the exiting nerve roots and the dural sac/traversing nerve roots can more accurately guide the selection of working cannula size and the design of new lumbar interbody fusion cage (Fig. 7), and can indirectly define the working "target" and safe area in one-stop percutaneous endoscopic transforaminal oblique fixation from posterior corner in lumbar spine (Figs. 6C, 6D). Theoretically, the positions where the 7.5-mm diameter cannula is tangent to the exiting nerve roots and the dural sac/traversing nerve roots in conventional transforaminal endoscopic surgery define the boundary of the actual safe area of Kambin's triangle. This is demonstrated by the green area in Fig. 8: the inner boundary is dural sac/traversing nerve roots, the outer-upper boundary is exiting nerve roots, the inner-upper boundary is the bone at the posterior-inferior corner of vertebral body, the outer-lower boundary is the outer surface of pedicle, and the inner-lower boundary is the bone at the posterior-superior corner of the vertebral body.

The ideal "target" for percutaneous endoscopic transforaminal oblique fixation from posterior corner in lumbar spine

In this paper, we measured the distances from the three preset targets to exiting nerve roots and dural sac/traversing nerve roots, as well as the distances from the exiting roots to the dural sac/traversing nerve roots in the upper and lower endplate planes in the coronal and sagittal planes of MRI images. We found that, except for P3 in L1/2, the mean distances from each target to the exiting and dural sac/traversing nerve roots in each segment of L1/2–L5/S1 were greater than the radius (3.75 mm) of conventional working cannula used in percutaneous endoscopic transforaminal surgery, which allows the placement of interbody fusion cages with cross-sectional diameters of no less than 7.5 mm. The distances from P1 to exiting nerve roots were significantly greater than those to the dural sac/traversing nerve roots (differences of 1–3 mm). The distances from P3 to exiting nerve roots were significantly smaller than those to the dural sac/traversing nerve roots (differences of 1–3 mm). However, the distances from P2 to exiting nerve roots and to dural sac/traversing nerve roots were similar in each segment (mean differences within 1 mm). Hence, P2 is the ideal "target" for percutaneous endoscopic transforaminal oblique fixation from posterior corner in lumbar spine, and the intersections between the vertical line 1/3 lateral from pedicle medial wall and the upper/lower endplates are the optimal points for screw placement.

In clinical practice of transforaminal endoscopic spine system (TESSYS), cannula was not introduced through the small external opening and corridor of Kambin's triangle. Instead, lumbar foraminoplasty was performed to grind the bone of superior articular process. Cannula was inserted directly through the

enlarged foramen to the inner opening of Kambin’s triangle. Larger working cannula can be used in segments to facilitate surgical operation, and the puncture point was far away from exiting nerve roots to reduce damage to exiting nerve roots and ganglions. Moreover, herniated and free nucleus pulposus can be removed, which is impossible with Yeung endoscopic spine system (YESS). Theoretically, the "optimal target or safe area" may shift inward in clinical practice due to Foraminoplasty, and contralateral decompression was reported by some spinal surgeons [35, 36]. We believe that one-stop complete decompression, fusion, and fixation in a single channel can be achieved in the near future with the development of spinal endoscopy technology and the emergence of minimally invasive integrated interbody fusion cages.

Further Research

Comparison between imaging measurement and dry bone measurement and correlation analysis between each index and body length will be performed in subsequent studies. In addition, objective evaluation of bearing capacity by biomechanical studies of compressive stress, stretch stress, torsion stress and fatigue load between lumbar vertebral bodies should be performed before the preparation of new endoscopic fusion cages. The established cage model matching with lumber vertebral body will be subjected to three-dimensional finite element analysis. Finally, the feasibility of one-stop percutaneous endoscopic transforaminal oblique fixation from posterior corner in lumbar spine will be preliminarily determined.

Conclusions

The intersection point between the vertical line from the medial 1/3 of pedicle and the horizontal midline of the posterior margin of intervertebral disc (P2) is an ideal "target" for oblique fixation from posterior corner in lumbar spine. Kambin’s triangle is not "safe". The actual safe area is smaller than theoretical prediction. The inner boundary is dural sac/traversing nerve roots, the outer-upper boundary is exiting nerve roots, the inner-upper boundary is the bone at the posterior-inferior corner of vertebral body, the outer-lower boundary is the outer surface of pedicle, and the inner-lower boundary is the bone at the posterior-superior corner of the vertebral body. The study shows that it is neuroanatomically feasible to perform one-stop complete decompression, fusion, and fixation in a single channel under spinal endoscopy. Further biomechanical studies and clinical trials are needed to determine whether oblique fixation from posterior corner in lumbar spine through Kambin’s triangle can be a new option for posterior spinal fusion.

Abbreviations

PE-TLIF: Percutaneous endoscopic transforaminal lumbar interbody fusion; Endo-LIF: Endoscopic transforaminal lumbar interbody fusion; MR: Magnetic Resonance; TESSYS: Transforaminal endoscopic spine system; YESS: Yeung endoscopic spine system.

Declarations

Ethics approval and consent to participate

Permission to conduct this retrospective study was obtained from the Hospital Ethics Committee.

Consent for publication

Not applicable

Availability of data and materials

The data used to support the findings of this study are available from the corresponding author upon request.

Competing interests

The authors declare that they have no competing interests.

Funding

The study received funding from key research and development program of Shandong Province: 2018GSF118074.

Authors' contributions

F-FC contributed to the research design, analysis of the data, and manuscript writing. J-X and C-S contributed to the acquisition and analysis of the data and wrote the program. X-YL and F-FC contributed to the acquisition and analysis of the data. J-MS contributed to the acquisition and analysis of the data. X-GC initiated and designed the study. All authors were fully involved in the study and approved the final version of this manuscript.

Acknowledgements

The authors sincerely acknowledge the entire staff of the Department of Spine, Shandong Provincial Hospital Affiliated to Shandong University, who offered assistance throughout the course of this study.

References

[1] Saraph V, Lerch C, Walochnik N, et al. Comparison of conventional versus minimally invasive extraperitoneal approach for anterior lumbar interbody fusion [J]. Eur Spine J, 2004, 13: 425-431.

[2] Zhang BX. Some problems in the treatment of lumbar with laminectomy [J]. Chinese journal of spine and spinal cord, 2004, 14 (10): 581-583.

[3] Khan NR, Clark AJ, Lee SL, et al. Surgical outcomes for minimally invasive vs open transforaminal lumbar interbody fusion: an updated systematic review and meta- analysis [J]. Neurosurgery, 2015,77 (6): 847-874.

[4] Yu HM, Yao XD, Lin JK, et al. Association between Low Back Pain and Paraspinal Muscle Change of One-level Transforaminal Lumbar Interbody Fusion：A Randomized Prospective Study of Minimally Invasive Procedure Versus Conventional Open Approach. Chinese and Foreign Medical Research, 2016, 14(33)：1-3.

[5] Watkins RG 4th, Hanna R, Chang D, et al. Sagittal alignment after lumbar interbody fusion: comparing anterior, lateral, and transforaminal approaches [J]. J Spinal Disord Tech, 2014, 27: 253-256.

[6] Hawasli AH, Khalifeh JM, Chatrath A, et al. Minimally invasive transforaminal lumbar interbody fusion with expandable versus static interbody devices: radiographic assessment of sagittal segmental and pelvic parameters [J]. Neurosurg Focus, 2017, 43 (2): E10.

[7] Yong Ahn, Myung Soo Youn & Dong Hwa Heo (2019) Endoscopic transforaminal lumbar interbody fusion: a comprehensive review, Expert Review of Medical Devices, 16:5, 373-380, DOI: 10.1080/17434440.2019.1610388.

[8] Stokes IA, Gardner-Morse M, Henry SM, Badger GJ. Decrease in trunk muscular response to perturbation with preactivation of lumbar spinal musculature. Spine (Phila Pa 1976), 2000, 25:1957-1964.

[9] Houten JK, Nasser R, Baxi N. Clinical assessment of percutaneous lumbar pedicle screw placement using the O-arm multidimensional surgical imaging system. Neurosurgery, 2012,70:990-995.

[10] Santos ER, Sembrano JN, Yson SC, Polly DW Jr. Comparison of open and percutaneous lumbar pedicle screw revision rate using 3-D image guidance and intraoperative CT. Orthopedics, 2015, 38: E129-134.

[11] Palmisani M, Gasbarrini A, Brodano GB, De Iure F, Cappuccio M, Boriani L, Amendola L, Boriani S. Minimally invasive percutaneous fixation in the treatment of thoracic and lumbar spine fractures. Eur Spine J, 2009, 18 Suppl 1:71-74.

[12] Wang ST, Ma HL, Liu CL, Yu WK, Chang MC, Chen TH. Is fusion necessary for surgically treated burst fractures of the thoracolumbar and lumbar spine: a prospective, randomized study? Spine (Phila Pa 1976), 2006, 31:2646-2652.

[13] Mobbs RJ, Raley DA. Complications with K-wire insertion for percutaneous pedicle screws. J Spinal Disord Tech, 2013, 27:390-394.

[14] Shen J. Fully endoscopic lumbar laminectomy and transforaminal lumbar interbody fusion under local anesthesia with conscious sedation: a case series[J]. World Neurosurg, 2019, 127: e745-750. DOI: 10.1016/j.wneu.2019.03.257.

[15] Heo DH, Park CK. Clinical results of percutaneous biportal endoscopic lumbar interbody fusion with application of enhanced recovery after surgery[J]. Neurosurg Focus, 2019, 46(4): E18.

[16] Nakamura S, Taguchi M. Full percutaneous lumbar interbody fusion: technical note[J]. J Neurol Surg A Cent Eur Neurosurg, 2017, 78(6):601-606.

[17] Morgenstern R, Morgenstern C. Percutaneous transforaminal lumbar interbody fusion with a posterolateral approach for the treatment of denegerative disk disease: feasibility and preliminary results[J]. Int J Spine Surg, 2015, 9:41.

[18] Zhang KH, Zhang WH, Xu BS, et al. CT-based Morphometric analysis of approach of percutaneous transforaminal endoscopic lumbar interbody fusion[J]. Orthop Surg, 2019, 11(2):212-220.

[19] Hardenbrook M, Lombardo S, Wilson MC, et al. The anatomic rationale for transforaminal endoscopic interbody fusion: a cadaveric analysis[J]. Neurosurg Focus, 2016, 40(2): E12.

[20] Ling Q, He E, Zhang H, et al. A novel narrow surface cage for full endoscopic oblique lateral lumbar interbody fusion: A finite element study[J]. J Orthop Sci, 2019, 24(6):991-998.

[21] Li ZZ, Hou SX, Shang WL, et al. Modified percutaneous lumbar foraminoplasty and percutaneous endoscopic lumbar discectomy: instrument design, technique notes, and 5 years follow-up[J]. Pain Physician, 2017, 20(1): E85-98.

[22] Li Z, Hou S, Shang W, et al. New instrument for percutaneous posterolateral lumbar foraminoplasty: case series of 134 with instrument design, surgical technique and outcomes[J]. Int J Clin Exp Med, 2015, 8(9):14672-14679.

[23] Jacquot F, Gastambide D. Percutaneous endoscopic transforaminal lumbar interbody fusion: is it worth it[J]? Int Orthop, 2013, 37(8):1507-1510.

[24] Ali Fahir Ozer, Tuncer Suzer, Halil Can, et al. Anatomic Assessment of Variations in Kambin's Triangle: A Surgical and Cadaver Study. World Neurosurg. (2017) 100:498-503.

[25] Kambin P, O'Brien E, Zhou L, et al. Arthroscopic microdiscectomy and selective Fragmentectomy[J]. Clin Orthop Relat Res,1998, (347):150-167.

[26] Mirkovic SR, Schwartz DQ, Glazier KD, et al. Anatomic considerations in lumbar posterolateral percutaneous procedures[J]. Spine,1995,30(18):1965-1971.

[27] Park JW, Nam HS, Cho SK, et al. Kambin's triangle approach of lumbar transforaminal epidural injection with spinal stenosis[J]. Ann Rehabil Med,2011,35(6):833-843.

[28] Luis M. Tumialán, Karthik Madhavan, Jakub Godzik, Michael Y. Wang. The History of and Controversy over Kambin's Triangle: A Historical Analysis of the Lumbar Transforaminal Corridor for

Endoscopic and Surgical Approaches[J]. World Neurosurgery,2019; 123: 402-408.

[29] Ozer AF, Suzer T, Can H, Falsafi M, Aydin M, Sasani M, et al. Anatomical assessment of variations in Kambin's triangle: a surgical and cadaver study. World Neurosurg. 2017; 100:498-503.

[30] Wang MY, Grossman J. Endoscopic minimally invasive transforaminal interbody fusion without general anesthesia: initial clinical experience with 1-year follow-up. Neurosurg Focus. 2016;40: E13.

[31] Vogelsang JP, Maier H. Clinical results and surgical technique for the treatment of extreme lateral lumbar disc herniations: the minimally invasive microscopically assisted percutaneous approach. Zentralbl Neurochir. 2008; 69:35-39.

[32] Schaffer JL, Kambin P. Percutaneous posterolateral lumbar discectomy and decompression with a 6.9-millimeter cannula. Analysis of operative failures and complications. J Bone Joint Surg Am. 1991; 73:822-831.

[33] Kim CW, Doerr TM, Luna IY, et al. Minimally invasive transforaminal lumbar interbody fusion using expandable technology: a clinical and radiographic analysis of 50 patients. World Neurosurg. 2016; 90:228-235.

[34] Hoshide R, Feldman E, Taylor W (February 02, 2016) Cadaveric Analysis of the Kambin's Triangle. Cureus 8(2): e475. DOI 10.7759/cureus.475

[35] Zhang B, Kong QQ, Feng P, Ma JS, Liu JL. Short-term effectiveness of percutaneous endoscopic transforaminal bilateral decompression for severe central lumbar spinal stenosis[J]. Chinese Journal of Reparative and Reconstructive Surgery, 2019,33(11):1399-1405.

[36] Xia MJ, Wang ZF, Chen T, et al. Treatment of lumbar spinal stenosis by full-endoscopic trephination-based bilateral decompression via a unilateral approach [J]. Chin J Clinicians (Electronic Edition), 2019,13(11):801-805.

Tables

Table 1. Distances from targets to ipsilateral exiting and dural sac/traversing nerve roots in the coronary plane (x± s, n=60, mm)

segment			L1/2	L2/3	L3/4	L4/5	L5/S1	P□
P1	c1	L	4.42±0.66	5.18±0.73	6.30±0.88	7.65±0.71	7.82±0.77	0.000
		R	4.35±0.44	5.07±0.67	5.84±0.77	7.61±0.55	7.42±1.02	0.000
		B*	4.39±0.53	5.13±0.70	6.08±0.83	7.63±0.63	7.62±0.91	0.000
	c2	L	3.52±0.49	4.23±0.74	4.67±0.37	5.52±0.53	4.64±0.54	0.000
		R	3.93±0.87	4.29±0.71	4.62±0.84	5.46±0.74	4.53±0.71	0.000
		B*	3.75±0.67	4.25±0.72	4.65±0.59	5.49±0.63	4.58±0.67	0.000
P2	c3	L	3.75±0.63	4.72±0.59	5.18±1.00	6.27±0.58	5.57±0.44	0.017
		R	4.27±0.93	4.65±0.77	5.17±0.86	6.09±0.93	5.41±0.72	0.023
		B*	4.03±0.77	4.69±0.66	5.17±0.93	6.18±0.90	5.49±0.55	0.021
	c4	L	3.93±0.75	4.43±0.70	5.37±1.09	6.54±0.68	6.34±0.91	0.000
		R	3.85±0.56	4.36±0.76	4.99±0.86	6.63±0.75	6.13±1.08	0.000
		B*	3.89±0.66	4.39±0.73	5.19±0.93	6.58±0.71	6.23±0.97	0.000
P3	c5	L	3.47±0.50	4.10±0.76	4.53±1.07	5.43±0.61	4.56±0.68	0.000
		R	3.81±0.78	4.19±0.64	4.56±0.77	5.35±0.94	4.43±0.34	0.000
		B*	3.67±0.61	4.16±0.43	4.54±0.88	5.39±0.78	4.49±0.59	0.000
	c6	L	4.51±0.67	5.82±0.37	6.04±1.00	7.92±0.91	7.57±0.77	0.000
		R	4.54±0.45	5.71±0.31	5.69±0.58	7.44±0.78	7.70±0.55	0.000
		B*	4.52±0.53	5.77±0.33	5.89±0.77	7.73±0.80	7.67±0.43	0.000

*p>0.05, there was no statistically significant difference between the two sides of each target in the same segment.

Table 2. Distances from the exiting nerve roots to the dural sac/traversing nerve roots in the upper and lower endplate planes in the coronary plane (x± s, n=60, mm)

segment		L1/2	L2/3	L3/4	L4/5	L5/S1	p□
d1	L	6.59±1.96	6.75±2.01	7.03±2.06	10.40±2.82	13.23±3.84	0.000
	R	6.51±1.92	6.63±2.22	7.11±2.47	10.17±2.86	13.44±4.33	0.000
	B*	6.55±1.93	6.69±2.11	7.07±2.21	10.28±2.84	13.38±3.97	0.000
d2	L	11.78±2.27	11.83±2.67	12.24±2.53	17.75±3.31	22.45±3.83	0.000
	R	11.72±2.19	11.90±2.53	12.09±2.13	18.21±3.61	21.64±4.01	0.000
	B*	11.75±2.23	11.90±2.53	12.15±2.37	17.93±3.46	22.03±3.92	0.000

*p>0.05, there was no statistically significant difference between the two sides of each target in the same segment.

Table 3. Distances from posterior-inferior (posterior-superior) corner of upper (lower) vertebral body to exiting nerve roots on the sagittal planes passing the targets (x± s, n=60, mm)

*p>0.05, there was no statistically significant difference between the two sides of each target in the same segment.†p<0.05, s2 in L5/S1 was statistically significant with other segments.

Figures

segment			L1/2	L2/3	L3/4	L4/5	L5/S1	p
P1	s1	L	3.33±0.74	3.42±0.23	3.47±1.01	3.60±0.56	4.76±1.07	0.000
		R	3.36±0.96	3.47±0.38	3.49±0.96	3.67±0.24	4.74±0.96	0.000
		B*	3.34±0.80	3.45±0.27	3.48±0.99	3.64±0.46	4.75±1.01	0.000
	s2	L	10.01±1.73	10.13±2.04	10.27±2.52	10.73±2.66	14.28±2.29†	0.000
		R	10.07±1.26	10.19±1.92	10.21±2.60	10.59±2.10	14.22±2.17†	0.000
		B*	10.04±1.51	10.15±1.99	10.25±2.56	10.66±2.50	14.25±2.22†	0.000
P2	s3	L	2.64±0.34	2.75±0.66	2.82±0.88	2.96±0.82	3.80±0.44	0.000
		R	2.67±0.55	2.70±0.68	2.89±0.22	2.90±0.97	3.87±0.57	0.000
		B*	2.65±0.47	2.72±0.67	2.86±0.69	2.93±0.89	3.83±0.49	0.000
	s4	L	7.92±0.73	8.07±1.13	8.19±1.46	8.69±1.01	11.63±3.20	0.000
		R	7.89±0.61	8.06±1.05	8.11±1.39	8.61±1.23	11.67±3.11	0.000
		B*	7.90±0.65	8.06±1.25	8.18±1.42	8.64±1.17	11.65±3.16	0.000
P3	s5	L	2.51±0.23	2.65±0.53	2.83±0.73	2.88±0.77	3.04±0.91	0.000
		R	2.52±0.24	2.64±0.66	2.87±0.55	2.81±0.21	3.11±0.73	0.000
		B*	2.51±0.24	2.64±0.59	2.85±0.64	2.85±0.37	3.07±0.82	0.000
	s6	L	7.51±0.69	7.96±1.03	8.44±1.33	8.50±0.92	9.11±1.93	0.000
		R	7.57±0.71	7.92±0.98	8.39±1.52	8.46±1.09	9.08±1.64	0.000
		B*	7.55±0.70	7.94±1.00	8.42±1.44	8.48±1.01	9.10±1.79	0.000

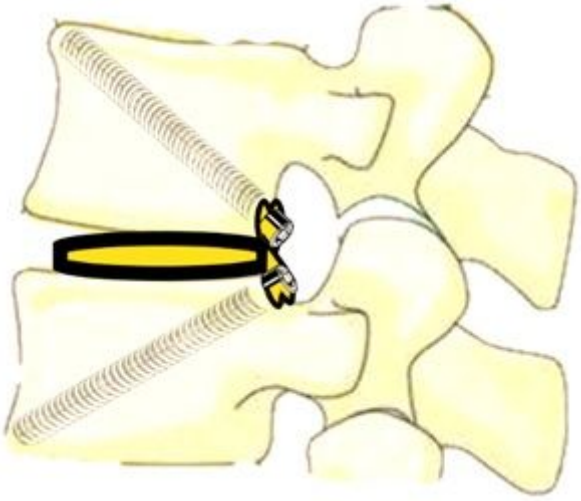

Figure 1

The working sketch of one-stop endoscopic fusion and fixation

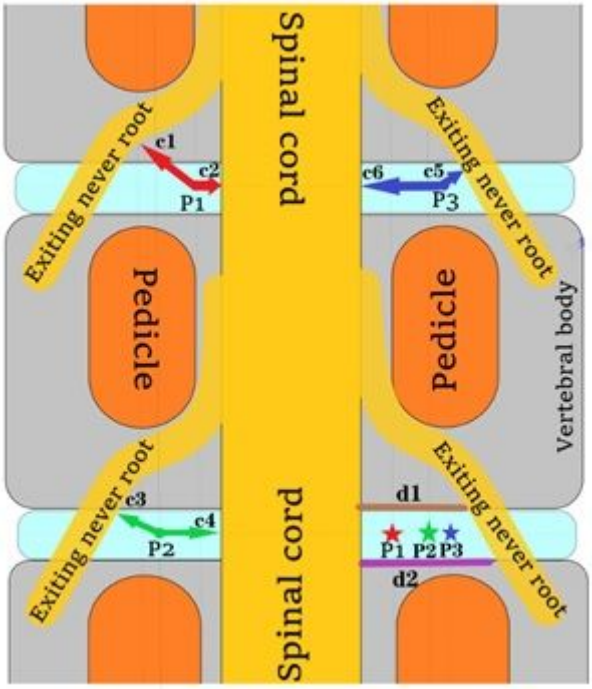

Figure 2

Measurement schematic diagram (c1, c2, c3, c4, c5, c6, d1, d2)

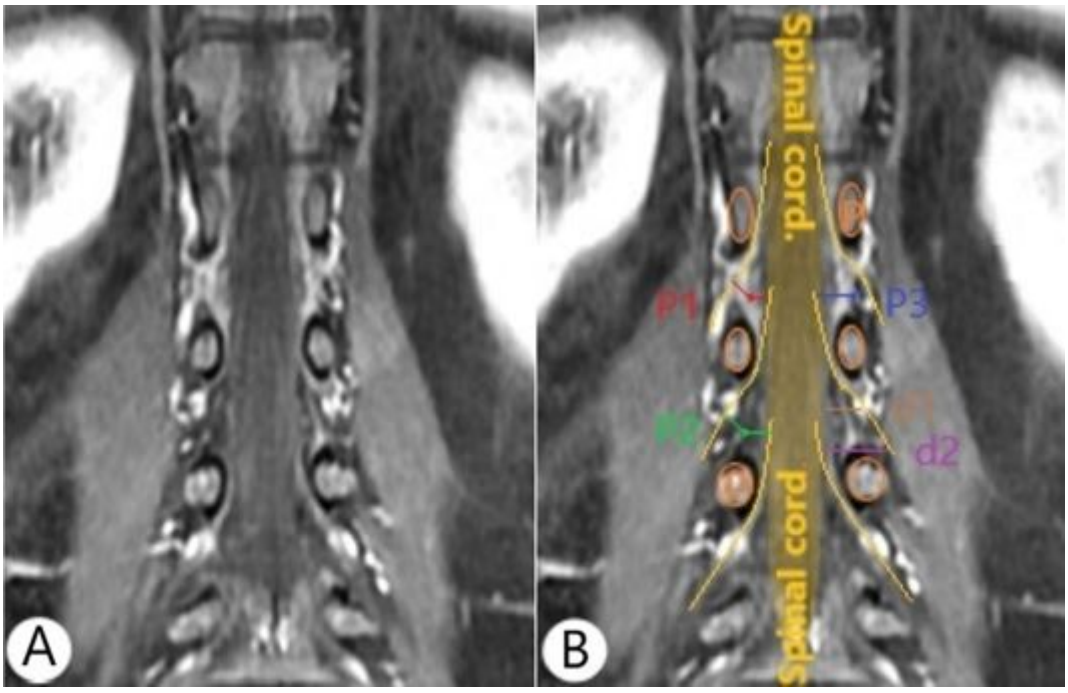

Figure 3

Actual measurements (c1, c2, c3, c4, c5, c6, d1, d2). A: Coronal image of lumbar spine in MRI; B: Data to be measured in A

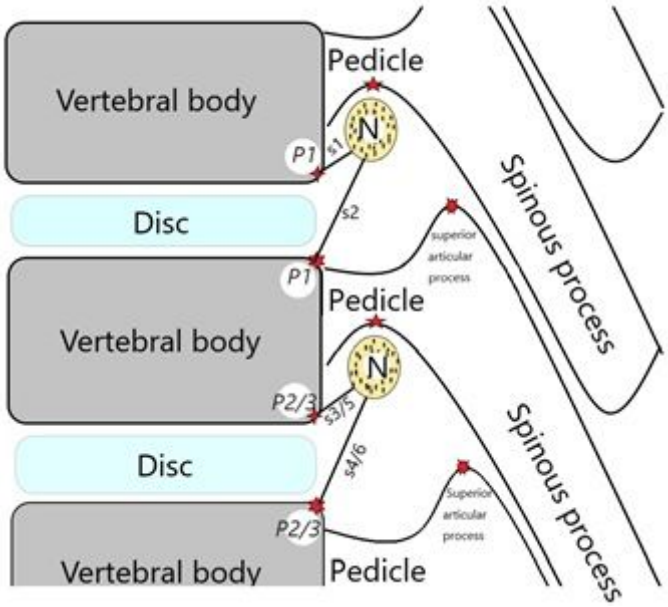

Figure 4

Measurement schematic diagram（s1, s2, s3, s4, s5, s6）

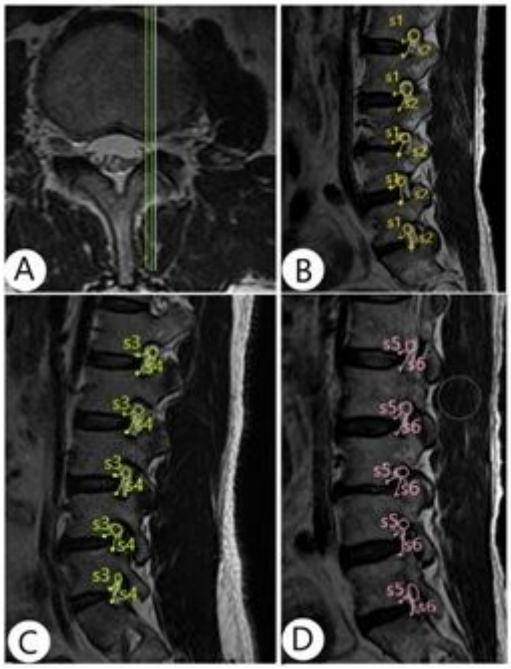

Figure 5

Actual measurements (s1, s2, s3, s4, s5, s6). A: P1, P2, P3 in axial plane. B: s1, s2 to be measured .C: s3, s4 to be measured. D: s5, s6 to be measured

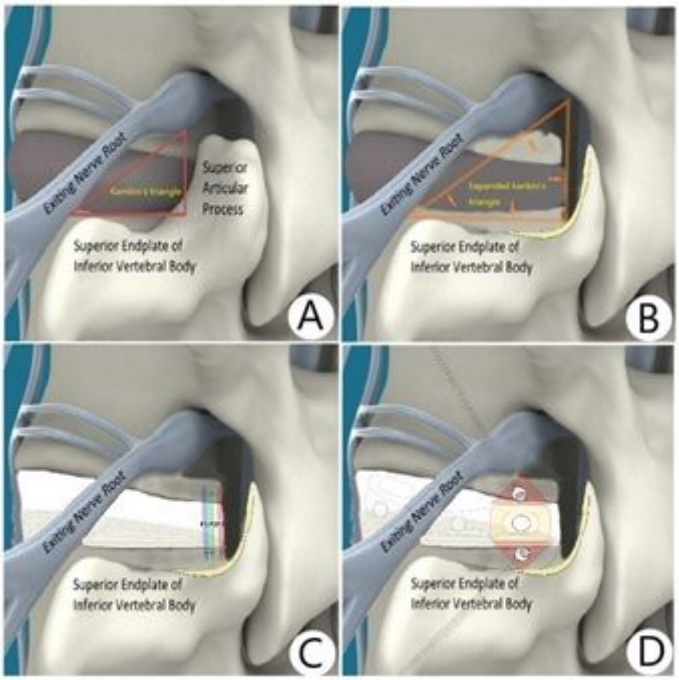

Figure 6

Application of Kambin's triangle in One-stop percutaneous endoscopic transforaminal oblique fixation from posterior corner in lumbar spine. A: Kambin's triangle before Foraminoplasty. B: Kambin's triangle after Foraminoplasty. C: Preset three points as targets. D: Effect picture of new lumbar interbody fusion cage

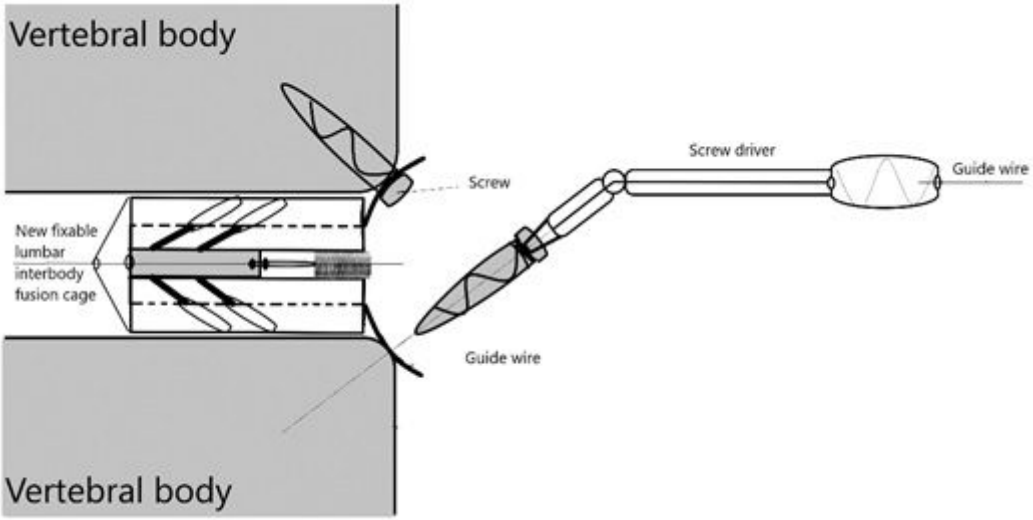

Figure 7

Structure schematic drawing of new fixable lumbar interbody fusion cage

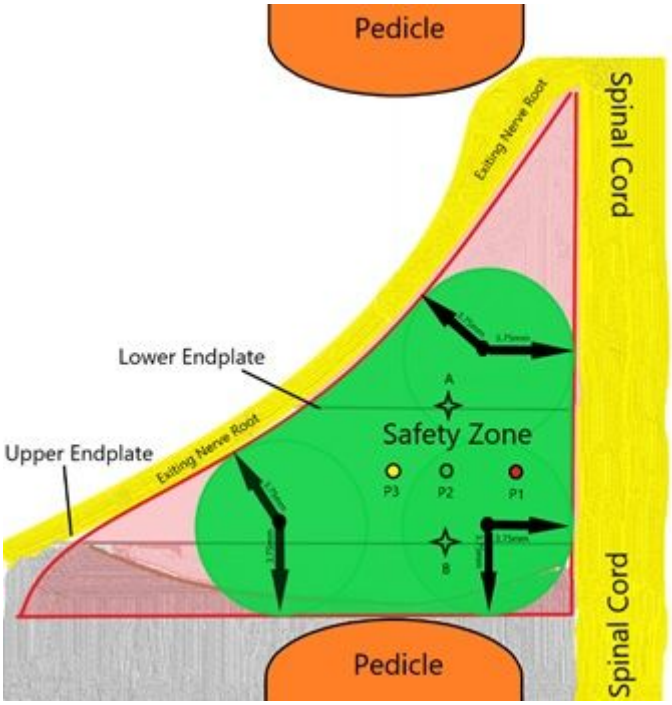

Figure 8

Actual work safety area in one-stop percutaneous endoscopic transforaminal oblique fixation from posterior corner in lumbar spine